Vietnam Journal of Science and Technology ***63*** *(3) (2024) 485-494*

doi:10.15625/2525-2518/18528

Zinc Oxide/Polypyrrole particle-decorated rod structure for NO_2 detection at low temperature

Vu Thanh Dong[1], Pham Tien Hung[2], Le Duc Anh[1], Ly Quoc Vuong[1], Dang Duy Khanh[1], Nguyen Thi Huong[1,*]

[1]*Institute of Chemistry and Materials, Academy of Military Science and Technology, 17 Hoang Sam, Nghia Do, Cau Giay, Ha Noi, Viet Nam*

[2]*Department of Physics, Le Quy Don Technical University, 236 Hoang Quoc Viet, Co Nhue, Bac Tu Liem, Ha Noi, Viet Nam*

[*]Email: *nguyenhuong0916@gmail.com*

Received: 15 July 2023; Accepted for publication: 15 April 2024

Abstract. In this study, zinc oxide (ZnO) nanoparticles with a size of about 50 - 70 nm were green-synthesized using tea leaves and ZnO/Polypyrrole (ZnO/Ppy) nanocomposites were obtained by ultrasonic-assisted chemical polymerization method using pyrrole monomer and the nanoparticles. The characterization of the materials was conducted using several analytical techniques, including Field Emission Scanning Electron Microscopy (FESEM), X-Ray Diffraction (XRD) and Ultraviolet visible spectrum (UV-Vis). The synthesized PPy material has a rod-shaped structure with diameters ranging from 100 to 200 nm. The ZnO/PPy nanocomposite system consists of PPy rods surrounded by ZnO particles. The gas sensing characteristics of the materials were also investigated by measuring their sensitivity, response time, and stability towards NO_2 at low temperatures and different humidities. Notably, the material exhibits considerable sensitivity to NO_2 gas at low temperatures with relatively rapid response and recovery times. Furthermore, a potential gas-sensing mechanism based on changes in the width of the depletion region is proposed.

Keywords: green synthesis, NO_2 gas sensor, ZnO, conductive polymer, low temperature.

Classification numbers: 2.4.2, 2.4.4, 2.9.4.

1. INTRODUCTION

The advancement of science and technology to improve human life is a global priority. However, rapid population growth and industrial expansion in sectors such as home appliances, transportation, and fossil fuels, while enhancing living standards, have also resulted in hazardous emissions that pose serious environmental risks [1]. Exposure to these pollutants has been associated with a range of health issues affecting the central nervous system, respiratory tract, and other organs, with symptoms such as bronchitis, headache, chest tightness, and vomiting commonly reported in cases of gas poisoning [2]. Consequently, the development of toxic gas detection sensors has become a major focus in advanced materials research to promote sustainable human development. Among various approaches - such as electrochemical, optical

fiber, and nanomaterial-based sensors - metal oxide semiconductor (MOS) sensors are particularly notable due to their straightforward synthesis, low cost, portability, and excellent sensitivity and selectivity without the need for auxiliary equipment. [3].

For chemo-resistive gas sensors based on MOS materials, zinc oxide (ZnO) is one of the potential materials due to its excellent physicochemical properties. The ZnO has a wide band gap of 3.37 eV and possesses several benefits, such as biocompatibility, chemical stability, environmental sustainability, and cost-effectiveness in synthesis [4]. It has a crystalline nature that enables the development of diverse nanostructures, including nanoparticles, namely one-dimensional (1D), two-dimensional (2D), and three-dimensional (3D) structures [5]. Previous studies have identified that the manipulation of material morphology affects the gas sensing ability of materials in the field of gas sensing research [6]. A key limitation of ZnO-based gas sensors remains their high operating temperature, which compromises longevity and precision. Recent research focuses on doped ZnO and heterostructures to enhance sensitivity/selectivity while lowering operational temperatures [7]. The combination of conductive polymers with ZnO, such as polypyrrole (PPy), is regarded as one of the recent and effective methods among these advanced approaches [8]. The changes in distribution and microstructural properties of polypyrrole after incorporating ZnO to enhance the sensing parameters of gas sensors were proven. For example, Harpale et al. (2020) synthesized a PPy-ZnO nanocomposite via electrochemical and SILAR methods, achieving an 82 % sensor response to 150 ppm NH_3 at 45 °C - significantly outperforming pristine ZnO and other sensors [9].

To the best of our knowledge, the investigation of ZnO/PPy-based gas sensors, especially the improvement of fabrication processes and gas selectivity enhancement, holds considerable promise for future development. Therefore, in the scope of this research, a green synthesis approach and chemical oxidation were employed to fabricate a ZnO/PPy nanocomposite material, followed by investigating the gas sensing characteristics of the sensor towards NO_2 gas. In particular, the ZnO nanoparticles were synthesized from green tea leaves and subsequently incorporated into a polymerization process involving pyrrole monomers.

2. MATERIALS AND METHODS

2.1. Materials

The following chemicals were used in our study: zinc acetate dihydrate ($Zn(CH_3COO)_2.2H_2O$, ≥ 98 %, Merck), methyl orange ($C_{14}H_{14}N_3NaO_3S$, ≥ 98 %, Macklin), iron(III) chloride ($FeCl_3$, ≥ 97 %, Merck), sodium hydroxide (NaOH, ≥ 98 %, Macklin), ethanol (C_2H_6O, ≥ 95 %, Macklin), pyrrole (C_4H_5N, 99 %, Macklin), ammonium hydroxide solution (NH_4OH, AR, 25 - 28 %, Macklin), and deionized water (H_2O). Tea leaves (*Camellia Sinensis*) were procured from Tan Cuong Xanh Company Limited at 42 Tay Son Street, Dong Da District, Ha Noi, Viet Nam. All leaves designated for extraction are 5 - 7 cm long and 2.5 - 4 cm wide.

2.2. Methods

2.2.1. Extraction process

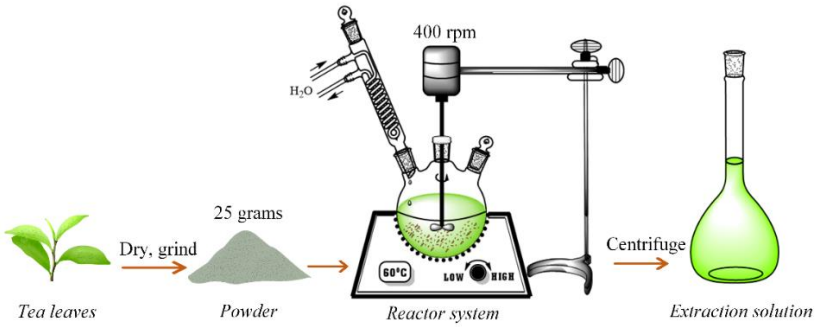

Figure 1. Tea extraction process.

The selected tea leaves are dried and ground into a fine powder. Subsequently, 25 grams of the powder are added to 500 mL of ethanol in the reactor system (Figure 1). The system is operated under controlled conditions with a stirring speed of 400 rpm and a temperature of 60 °C for 2 hours. The dark green solution is then centrifuged at 10,000 rpm for 5 minutes to separate the powder from the solution. The resulting solution is then stored at 5 ^{o}C in a refrigerator.

2.2.2. Synthesis process of ZnO nanoparticles

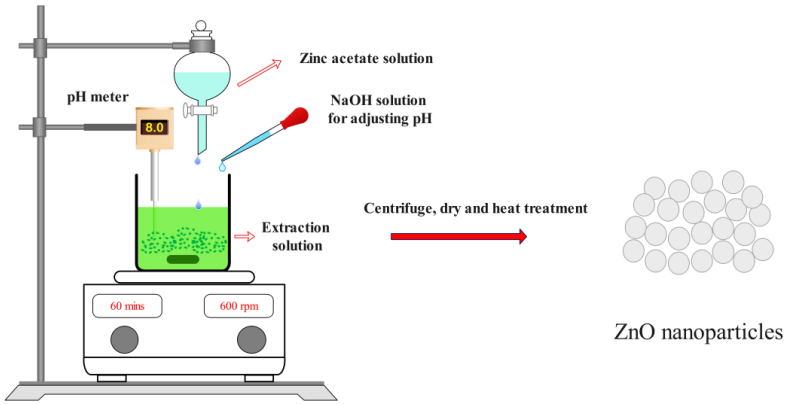

Figure 2. Synthesis process of ZnO nanoparticles.

The synthesis of ZnO nanoparticles follows an approach similar to that described in our previous research [10]. 2 grams of $Zn(CH_3COO)_2.2H_2O$ were dissolved in 20 mL of distilled water. The resulting solution was then dropwise added to a 100 mL flask containing the prepared extraction solution. The entire solution was placed on a magnetic stirrer at 600 rpm and maintained at a pH of 8 with 1 M NaOH solution. The stirring process was carried out for 60 minutes. After the reaction, the solution was centrifuged to collect the precipitate, which was dried overnight at 60 °C. Finally, the obtained powder was calcined at 600 °C for 3 hours.

2.2.3. Synthesis process of ZnO/PPy nanocomposites

0.1 gram of $C_{14}H_{14}N_3NaO_3S$ was added to 60 mL of distilled water and the solution was stirred at room temperature. Then, 0.5 grams of $FeCl_3$ were quickly added to the solution. Subsequently, 0.035 grams of ZnO nanoparticles were added, and the mixture was sonicated for an hour. A dark red solution was obtained, to which 0.362 mL of C_4H_5N were added and the solution was stirred for 24 hours. The resulting mixture was dried overnight at 60 °C.

2.2.4. Characterizations

The morphological properties of the materials were determined using an S-4800 field emission scanning electron microscope (FESEM, Hitachi, Japan), operating at a voltage of 3.0 kV under ambient conditions. The crystal structure characteristics of the materials were determined using an X-ray diffractometer (D8 Advance, BRUKER AXS, Germany) with CuKα radiation at 50 kV. The UV–vis spectra were recorded using a Shimadzu UV-1800 double-beam UV/Vis scanning spectrophotometer from Japan.

2.2.5. Gas sensing experiment

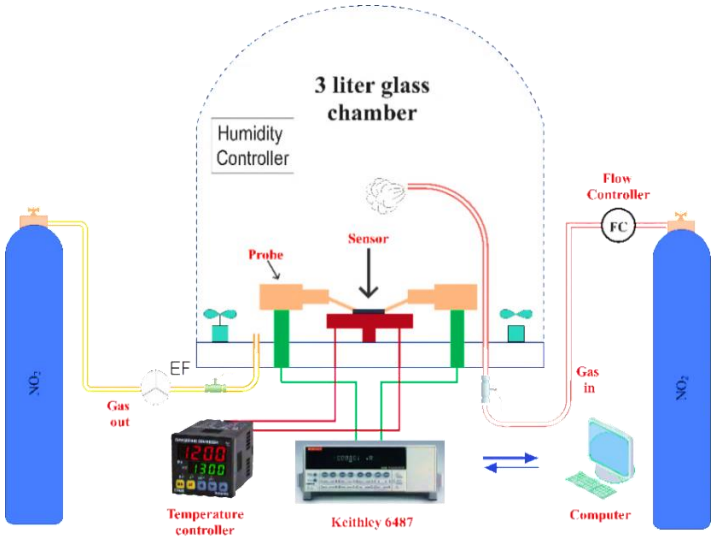

Figure 3. Schematic diagram of the gas sensing experiment.

The gas sensor was prepared by drop-casting a suspension of ZnO/PPy material in ethanol on an electrode, which was dried at 60 ^{o}C before conducting gas sensing experiments. Measurements were performed using a computer-connected system and Keithley 6487 equipment at the School of Engineering Physics, Hanoi University of Science and Technology (Figure 3). The operating temperature of the sensor was maintained at a stable 40 ^{o}C using a temperature controller. The humidity control during the measurement was achieved by a DQ 300 TRH 96 humidity controller. The sensor response was quantified using the equation $S = R_a/R_g$, where R_a and R_g represent the sensor resistances in air and in NO_2 oxidizing gas, respectively. The response time was defined as the duration required for the sensor to reach 90 % of its saturation resistance after exposure to NO_2. Similarly, the recovery time was defined as the duration needed for the sensor to return to 90 % of its initial resistance value after being exposed to air.

3. RESULTS AND DISCUSSION

3.1. Materials characteration

Figures 4a, 4b, and 4c depict the morphological characteristics of three distinct materials: ZnO, PPy, and the ZnO/PPy nanocomposite material, in a sequential manner. The ZnO

nanoparticles in Figure 4a. display a relatively homogeneous size distribution, spanning from 50 to 70 nm. On the other hand, the synthesized PPy material exhibits a rod-shaped structure, characterised by a diameter ranging from approximately 100 to 200 nm. Figure 4c demonstrates the ZnO/PPy nanocomposite system, consisting of PPy rods surrounded by ZnO particles.

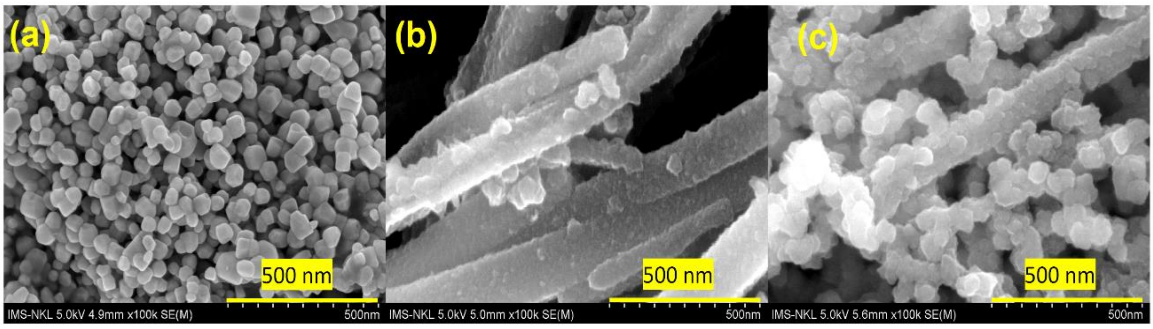

Figure 4. FESEM images of ZnO (a), PPy (b), and ZnO/PPy (c).

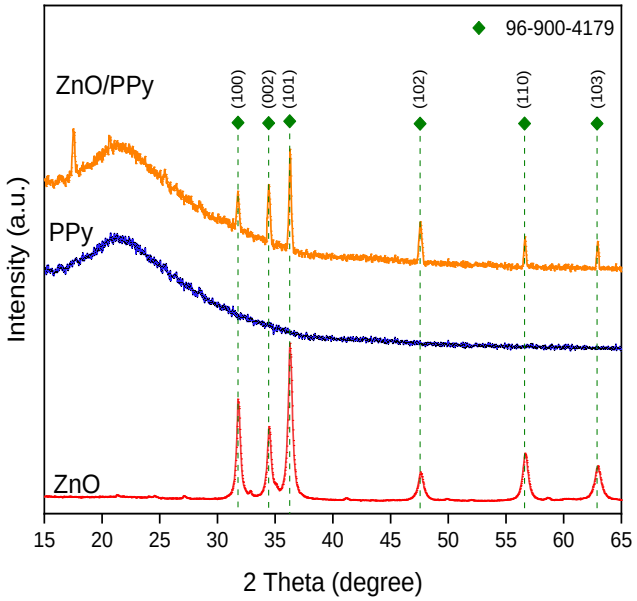

Figure 5. X-ray diffraction spectrum of materials.

The phase structures of ZnO, PPy, and ZnO/PPy materials are shown in Figure 5. Based on the intensity and characteristics of the peaks, the ZnO nanoparticles were found to be highly crystalline while the polypyrrole phase was found to be amorphous [11]. The phase structure of the synthesized ZnO material exhibited a hexagonal shape, with characteristic peaks observed at positions corresponding to lattice planes (100), (002), (101), (102), (110), and (103) as referenced to COD 96-900-4179. Additionally, the ZnO/PPy composite material displayed much weaker peak signals than ZnO nanoparticles, which may be attributed to the low ZnO content in the composite. The signal at the broad peak at $2\theta = 20.530^{o}$ of the composite also indicated the presence of PPy [12] while the strange peak at around 17^{o} may be attributed to the formation of $Zn(OH)_2$ during the reaction process without heat treatment [13].

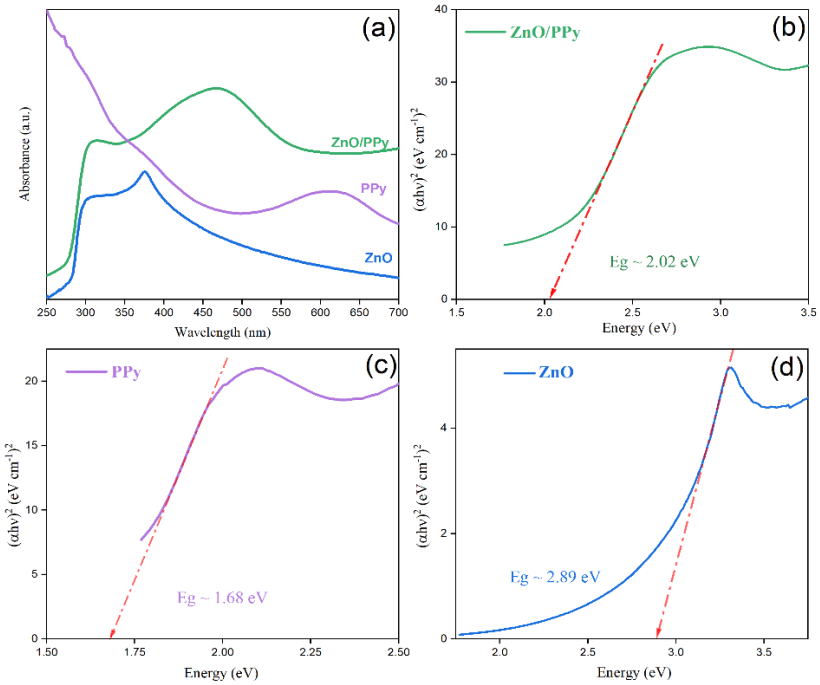

Figure 6. UV-Vis absorption spectra of ZnO, ZnO/PPy, PPy (a) and band gap of ZnO/PPy nanocomposite (b), PPy (c) and ZnO (d).

Figure 6a displays the UV-Vis spectra of ZnO NPs (blue line), PPy rods (violet line) and ZnO/PPy nanocomposites (green line). Considering these data, the energy band gap (E_g) of these three materials was caculated using the Tauc method [14]. The E_g of ZnO NPs is typically greater than 3.2 eV [15]; however, in this study, the E_g of ZnO NPs is approximately 2.89 eV (Figure 6d). According to Mansoob Khan *et al.*, the reduction of the E_g is due to the modification of the surface with the functional groups from plant leaf extracts [16]. Additionally, the estimated E_g of the PPy rods and ZnO/PPy nanocomposites are approximately 1.68 eV and 2.02 eV, respectively (Figures 6b, 6c). This result demonstrates a significant reduction in the E_g of ZnO upon the modification with PPy, consistent with several previous publications [17, 18].

3.2. Gas sensing properties

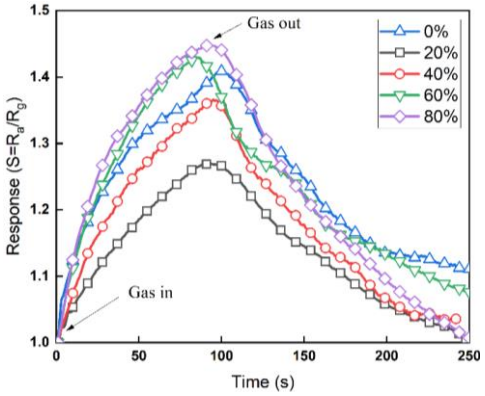

Figure 7. Relationship between sensitivity and humidity level.

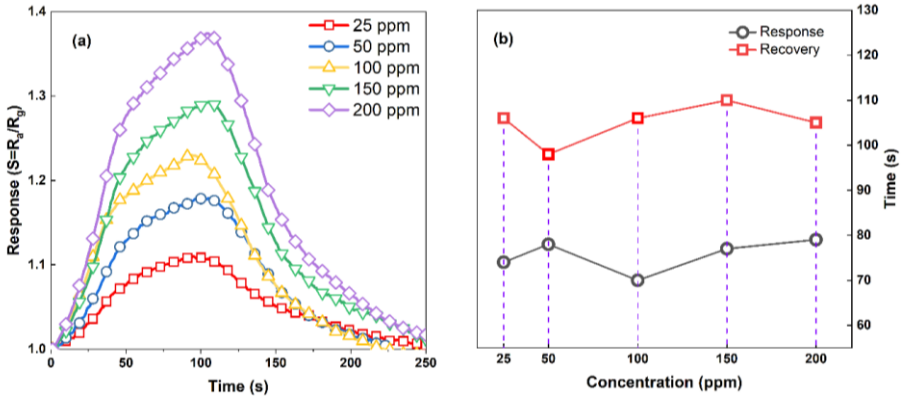

Figure 8. Gas response of ZnO/Ppy (a) and sensor's response and recovery time (b) at different concentrations.

The impact of humidity on the gas sensitivity of the material was investigated at different humidity levels at 200 ppm NO_2 (Figure 7). When the humidity level was at 0 %, the numerical value of S was approximately 1.4089. When subjected to low humidity levels ranging from 20 % to 40 %, the observed values of S exhibited a significant decrease, reaching approximately 1.364 and 1.268. The observed decline can be attributed to the competitive adsorption phenomenon between NO_2 gas and water [19]. Conversely, under high humidity conditions, the magnitude of S exhibited an increase in a low-moisture atmosphere, specifically reaching approximately 1.428 at a humidity level of 60 % and 1.447 at a humidity level of 80 %. It is hypothesized that under low-temperature conditions, the adsorption of many water molecules will occur on the surface of the composite material coated predominantly with ZnO nanoparticles. When the material interacts with NO_2 gas, the gas molecules will displace water molecules from the material's surface, resulting in a change in resistance and increased sensitivity [20].

After experimenting to assess the influence of humidity, the sensor was preserved in a vacuum environment for one day. Subsequently, the impact of NO_2 gas concentration was further investigated at 25, 50, 100, 150, and 200 ppm at 80 % humidity (Figure 8a). In general, the sensor's sensitivity increases consistently as the concentration of NO_2 increases. Among them, the highest sensitivity values at concentrations of 25, 50, 100, 150, and 200 ppm are 1.110, 1.179, 1.230, 1.292, and 1.374, respectively. Figure 8b illustrates that the sensor exhibits significantly faster response time than the recovery time at each NO_2 concentration (approximately 20 to 30 seconds).

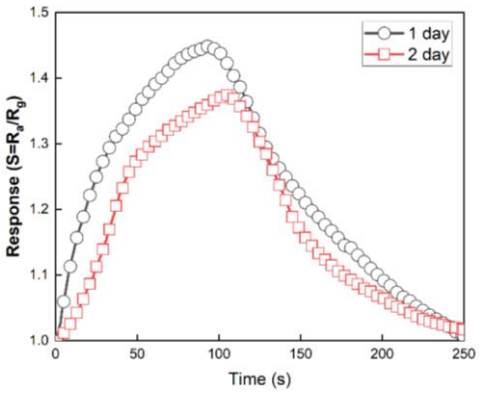

Figure 9. Assessment of sensor stability.

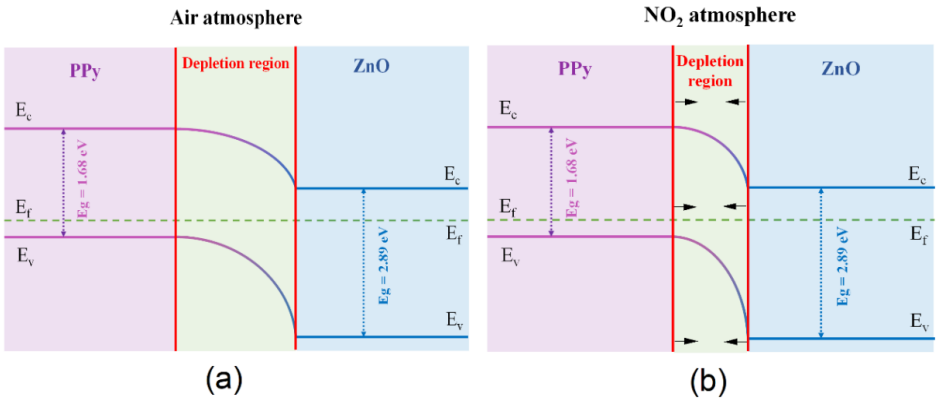

Figure 10. Schematic diagram of energy band for ZnO/PPy nanocomposites in air atmosphere (a) and NO_2 atmosphere (b).

The sensor's stability was evaluated under varying humidity and NO_2 concentrations, as shown in Figure 9. After one day at 200 ppm NO_2 and 80 % humidity, the highest sensitivity decreased slightly from 1.445 to 1.374, with only minor changes observed in response and recovery times. The NO_2 sensing mechanism of the nanocomposites is depicted schematically in Figure 10(a–b). The Fermi energy level (Ef) of polypyrrole is situated near the valence band since it behaves as a p-type semiconductor [21]. In contrast, the ZnO NPs are categorized as an n-type semiconductor [22], so its Fermi energy level is close to the conduction band. The nanocomposites exhibit p-n junction properties and depletion region formation as shown in Figure 10a. Notably, NO_2 exposure reduces electrical resistance, confirming p-type dominance and PPy-mediated charge transport. Previous studies have affirmed that the interaction between NO_2 gas molecules and the π-electron networks of PPy leads to a decrease in resistance [23, 24]. Therefore, the width of the depletion region decreased (Figure 10b), facilitating the detection of small quantities of NO_2 gas molecules.

4. CONCLUSIONS

ZnO nanoparticles were synthesized using a green approach, in which green tea leaves were employed as the reaction agent. The gas sensitivity of the nanocomposite material based on polypyrrole rod-likestructure with ZnO nanoparticles adhered onto its surface was investigated at room temperature. The highest sensitivity value for 25 ppm NO_2 at a temperature of 40 °C and 80 % humidity was 1.109, while for 200 ppm NO_2 under similar conditions the highest sensitivity value was 1.445. The response time ranged from 70 to 80 seconds, and the recovery time ranged from 100 to 110 seconds at different NO_2 concentrations. In general, ZnO/PPy is a promising material for NO_2 gas sensors; however, the stability, response time and recovery time of the nanocomposites towards NO_2 also need to be improved in further studies.

Acknowledgements. This research is funded by the basic research grant from the Institute of Chemistry and Materials titled "Green synthesis of ZnO/conductive polymer for oriented application in the detection of toxic gases at defense production facilities" starting from March 2023.

CRediT authorship contribution statement. Vu Thanh Dong, Pham Tien Hung: Methodology, Investigation, Funding acquisition. Le Duc Anh, Dang Duy Khanh: Formal analysis. Ly Quoc Vuong, Nguyen Thi Huong: Formal analysis, Supervision.

Declaration of competing interest. The authors declare that they have no known competing financial interests or personal relationships that could have appeared to influence the work reported in this paper.

REFERENCES

1. Dhall S., Mehta B. R., Tyagi A. K., and Sood K. - A review on environmental gas sensors: Materials and Technologies, Sens Int. **2** (2021) 100116. https://doi.org/10.1016/j.sintl. 2021.100116
2. Li A. J., Pal V. K., and Kannan K. - A review of environmental occurrence, toxicity, biotransformation and biomonitoring of volatile organic compounds, Environ Toxicol Chem. **3** (2021) 91-116. https://doi.org/10.1016/j.enceco.2021.01.001
3. Krishna K. G., Parne S., Pothukanuri N., Kathirvelu V., Gandi S., and Joshi D. - Nanostructured metal oxide semiconductor-based gas sensors: A comprehensive review. Sens Actuators a Phys. **341** (2022) 113578. https://doi.org/10.1016/j.sna.2022.113578
4. Bhati V. S., Hojamberdiev M., and Kumar M. - Enhanced sensing performance of ZnO nanostructures-based gas sensors: A review, Energy Rep. **6** (2020) 46-62. https://doi.org/ 10.1016/j.egyr.2019.08.070
5. Zhang B., Li M., Song Z., Kan H., Yu H., Liu Q., Zhang G., and Liu H. - Sensitive H2S gas sensors employing colloidal zinc oxide quantum dots, Sens Actuators B Chem. **249** (2017) 558-563. https://doi.org/10.1016/j.snb.2017.03.098
6. Kang Y., Yu F., Zhang L., Wang W., Chen L., and Li Y. - Review of ZnO-based nanomaterials in gas sensors, Solid State Ionics **360** (2021) 115544. https://doi.org/ 10.1016/j.ssi.2020.115544
7. Franco M. A., Conti P. P., Andre R. S., and Correa D. S. - A review on chemiresistive ZnO gas sensors, Sens. Actuators Rep. **4** (2022) 100100. https://doi.org/ 10.1016/j.snr.2022.100100
8. Zhang C., Luo Y., Xu J., and Debliquy M. - Room temperature conductive type metal oxide semiconductor gas sensors for NO2 detection, Sens Actuators a Phys. **289** (2019) 118-133. https://doi.org/10.1016/j.sna.2019.02.027
9. Harpale K., P. Kolhe, P. Bankar, R. Khare, S. Patil, N. Maiti, M.G. Chaskar, M.A. More, and K.M. Sonawane. - Multifunctional characteristics of polypyrrole-zinc oxide (PPy-ZnO) nanocomposite: Field emission investigations and gas sensing application, Synth. Met. **269** (2020): p. 116542. https://doi.org/10.1016/j.synthmet.2020.116542
10. Pham T. M. H., Vu M. T., Cong T. D., Nguyen N. S., Doan T. A., Truong T. T., and Nguyen T. H. - Green sonochemical process for preparation of polyethylene glycol-Fe3O4/ZnO magnetic nanocomposite using rambutan peel extract as photocatalyst, for removal of methylene blue in solution, Bull. Mater. Sci. **45** (1) (2022) 13. https://doi.org/ 10.1007/s12034-021-02584-2
11. Pirsa S., Shamusi T., and Kia E. M. - Smart films based on bacterial cellulose nanofibers modified by conductive polypyrrole and zinc oxide nanoparticles, J. Appl. Polym. Sci. **135** (34) (2018) 46617. https://doi.org/10.1002/app.46617
12. Shrikrushna S., Kher J. A., Kulkarni M. V. J. J. O. N., and Nanotechnology - Influence of dodecylbenzene sulfonic acid doping on structural, morphological, electrical and optical properties on polypyrrole/3C-SiC nanocomposites, J. Nanomed. Nanotechnol **6** (5) (2015) 1. https://doi.org/10.4172/2157-7439.1000313
13. Hussain A., Shumaila A. Dhillon I. Sulania and Siddiqui A. M. - Comparative Study of Polypyrrole/Zinc Oxide Nanocomposites Synthesized by Different Methods, In:

Proceedings of the International Conference on Atomic, Molecular, Optical & Nano Physics with Applications, Singapore, 2022. pp. 601-607

14. Haryński Ł., Olejnik A., Grochowska K., and Siuzdak K. - A facile method for Tauc exponent and corresponding electronic transitions determination in semiconductors directly from UV–Vis spectroscopy data, Opt. Mater. **127** (2022) 112205. https://doi.org/10.1016/j.optmat.2022.112205
15. Hjiri M., Bahanan F., Aida M.S., El Mir L., and Neri G. - High Performance CO Gas Sensor Based on ZnO Nanoparticles, J. Inorg. Organomet. Polym. Mater. **30** (10) (2020) 4063-4071. https://doi.org/10.1007/s10904-020-01553-2
16. Khan M. M., Saadah N. H., Khan M. E., Harunsani M. H., Tan A. L., and Cho M. H. - Potentials of Costus woodsonii leaf extract in producing narrow band gap ZnO nanoparticles, Mater. Sci. Semicond. Process **91** (2019) 194-200. https://doi.org/10.1016/j.mssp.2018.11.030
17. Chougule M. A., Sen S., and Patil V. B. - Polypyrrole–ZnO hybrid sensor: Effect of camphor sulfonic acid doping on physical and gas sensing properties, Synth. Met. **162** (17) (2012) 1598-1603. https://doi.org/10.1016/j.synthmet.2012.07.002
18. Balakumar V. and Baishnisha A. - Rapid visible light photocatalytic reduction of Cr6+ in aqueous environment using ZnO-PPy nanocomposite synthesized through ultrasonic assisted method, Surf. Interfaces **23** (2021) 100958. https://doi.org/10.1016/j.surfin.2021.100958
19. Duoc V. T., Hung C. M., Nguyen H., Duy N. V., Hieu N. V., and Hoa N. D. - Room temperature highly toxic NO2 gas sensors based on rootstock/scion nanowires of SnO2/ZnO, ZnO/SnO2, SnO2/SnO2 and, ZnO/ZnO, Sens Actuators B Chem. **348** (2021) 130652. https://doi.org/10.1016/j.snb.2021.130652
20. Liu B., Liu X., Yuan Z., Jiang Y., Su Y., Ma J., and Tai H. - A flexible NO2 gas sensor based on polypyrrole/nitrogen-doped multiwall carbon nanotube operating at room temperature, Sens Actuators B Chem. **295** (2019) 86-92. https://doi.org/10.1016/j.snb.2019.05.065
21. Das M. and Roy S. - Polypyrrole and associated hybrid nanocomposites as chemiresistive gas sensors: A comprehensive review, Mater. Sci. Semicond. Process. **121** (2021) 105332. https://doi.org/10.1016/j.mssp.2020.105332
22. Li G., Sun Z., Zhang D., Xu Q., Meng L., and Qin Y. - Mechanism of Sensitivity Enhancement of a ZnO Nanofilm Gas Sensor by UV Light Illumination, ACS Sensors **4** (6) (2019) 1577-1585. https://doi.org/10.1021/acssensors.9b00259
23. Mane A. T., Navale S. T., Sen S., Aswal D. K., Gupta S. K., and Patil V. B. - Nitrogen dioxide (NO2) sensing performance of p-polypyrrole/n-tungsten oxide hybrid nanocomposites at room temperature, Org. Electron. **16** (2015) 195-204. https://doi.org/10.1016/j.orgel.2014.10.045
24. Nellaiappan S., Shalini Devi K. S., Selvaraj S., Krishnan U. M., and Yakhmi J. V. - Chemical, Gas and Optical Sensors Based on Conducting Polymers, in Advances in Hybrid Conducting Polymer Technology, S. Shahabuddin, *et al.* (Editors), Springer International Publishing, Cham., 2021, pp. 159-200.